Inorg. Chem. **2009**, *48*, 4514−4523

Effects of Electron-Deficient β-Diketiminate and Formazan Supporting Ligands on Copper(I)-Mediated Dioxygen Activation

Sungjun Hong,[†] Lyndal M. R. Hill,[†] Aalo K. Gupta,[†] Benjamin D. Naab,[†] Joe B. Gilroy,[‡] Robin G. Hicks,*[,‡] Christopher J. Cramer,*[,†] and William B. Tolman*[,†]

Department of Chemistry, Center for Metals in Biocatalysis, and Supercomputing Institute, University of Minnesota, 207 Pleasant St. SE, Minneapolis, Minnesota 55455, and Department of Chemistry, University of Victoria, P.O. Box 3065, Victoria, British Columbia, Canada V8W 3V6

Received February 5, 2009

Copper(I) complexes of a diketiminate featuring CF_3 groups on the backbone and dimethylphenyl substituents (**4**) and a nitroformazan (**5**) were synthesized and shown by spectroscopy, X-ray crystallography, cyclic voltammetry, and theory to contain copper(I) sites electron-deficient relative to those supported by previously studied diketiminate complexes comprising alkyl or aryl backbone substituents. Despite their electron-poor nature, oxygenation of $LCu(CH_3CN)$ (L = **4** or **5**) at room temperature yielded bis(hydroxo)dicopper(II) compounds and at −80 °C yielded bis(μ-oxo)dicopper complexes that were identified on the basis of UV−vis and resonance Raman spectroscopy, spectrophotometric titration results (2:1 Cu/O_2 ratio), electron paramagnetic resonance spectroscopy (silent), and density functional theory calculations. The bis(μ-oxo)dicopper complex supported by **5** exhibited unusual spectroscopic properties and decayed via a novel intermediate proposed to be a metallaverdazyl radical complex, findings that highlight the potential for the formazan ligand to exhibit "noninnocent" behavior.

Introduction

The binding and activation of dioxygen by Cu ions is central to the function of numerous biological and synthetically useful catalytic systems.[1] In efforts to understand the underlying chemistry, studies of the O_2 reactivity of copper(I) complexes with a variety of supporting ligand types have been performed.[2] These studies have led to the identification of copper−oxygen intermediates with diverse nuclearities, topologies, and redox states and to the discovery of structure/reactivity correlations relevant to biological and other catalytic processes. Despite this progress, much remains to be learned, particularly about how the nature of supporting ligand(s) influences the structures and properties of copper−oxygen intermediates. Previously, ligand denticity, steric profile, and electronic properties were shown to be important determinants, with notable emphasis having been placed on evaluating how these factors control the relative stability of interconverting peroxo- and bis(μ-oxo)dicopper isomers.[2,3]

In prior work, we focused our attention on the O_2 reactivity of copper(I) complexes of strongly electron-donating, monoanionic, and bidentate diketiminate (and anilidoimine)[4] ligands, the steric properties of which can be manipulated readily through variation of substituents R, R′, and/or R″ (Figure 1, top). For most of the diketiminate ligands, bis(μ-oxo)dicopper

* To whom correspondence should be addressed. E-mail: rhicks@uvic.ca (R.G.H.), cramer@umn.edu (C.J.C.), wtolman@umn.edu (W.B.T.).
† University of Minnesota.
‡ University of Victoria.

(1) Selected recent reviews: (a) Solomon, E. I.; Chen, P.; Metz, M.; Lee, S.-K.; Palmer, A. E. *Angew. Chem., Int. Ed.* **2001**, *40*, 4570–4590. (b) Solomon, E.; Sarangi, R.; Woertink, J.; Augustine, A.; Yoon, J.; Ghosh, S. *Acc. Chem. Res.* **2007**, *40*, 581–591. (c) Klinman, J. P. *J. Biol. Chem.* **2006**, *281*, 3013–3016. (d) Arends, I.; Gamez, P.; Sheldon, R. A. *Adv. Inorg. Chem.* **2006**, *58*, 235–279. (e) Battaini, G.; Granata, A.; Monzani, E.; Gullotti, M.; Casella, L. *Adv. Inorg. Chem.* **2006**, *58*, 185–233. (f) Punniyamurthy, T.; Rout, L. *Coord. Chem. Rev.* **2008**, *252*, 134–154.

(2) Selected recent reviews:(a) Lewis, E. A.; Tolman, W. B. *Chem. Rev.* **2004**, *104*, 1047–1076. (b) Mirica, L. M.; Ottenwaelder, X.; Stack, T. D. P. *Chem. Rev.* **2004**, *104*, 1013–1045. (c) Hatcher, L. Q.; Karlin, K. D. *Adv. Inorg. Chem.* **2006**, *58*, 131–184. (d) Hatcher, L.; Karlin, K. D. *J. Biol. Inorg. Chem.* **2004**, *9*, 669–683. (e) Itoh, S. *Curr. Opin. Chem. Biol.* **2006**, *10*, 115–122. (f) Cramer, C. J.; Tolman, W. B. *Acc. Chem. Res.* **2007**, *40*, 601–608. (g) Suzuki, M. *Acc. Chem. Res.* **2007**, *40*, 609–617.

(3) For example, see:(a) Cole, A. P.; Mahadevan, V.; Mirica, L. M.; Ottenwaelder, X.; Stack, T. D. P. *Inorg. Chem.* **2005**, *44*, 7345–7364. (b) Stack, T. D. P. *Dalton Trans.* **2003**, 1881–1889. (c) Lam, B. M. T.; Halfen, J. A.; Young, V. G., Jr.; Hagadorn, J. R.; Holland, P. L.; Lledós, A.; Cucurull-Sánchez, L.; Novoa, J. J.; Alvarez, S.; Tolman, W. B. *Inorg. Chem.* **2000**, *39*, 4059–4072. (d) Hatcher, L. Q.; Vance, M. A.; Narducci Sarjeant, A. A.; Solomon, E. I.; Karlin, K. D. *Inorg. Chem.* **2006**, *45*, 3004–3013.

(4) Reynolds, A. M.; Gherman, B. F.; Cramer, C. J.; Tolman, W. B. *Inorg. Chem.* **2005**, *44*, 6989–6997.

10.1021/ic9002466 CCC: $40.75
Published on Web 04/07/2009

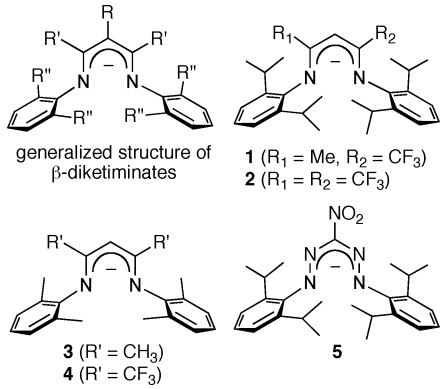

Figure 1. Diketiminate and formazan (**5**) ligands.

complexes were observed,[5] whereas the highly hindered variants having R″ = iPr and R′ = Me or tBu enabled characterization of a side-on monocopper−dioxygen adduct.[2f,5a,6] Detailed spectroscopic and theoretical studies showed that this adduct is best described as a copper(III) peroxide as a result of the powerful electron donation of the diketiminate ligand.[6,7] Calculations also showed, however, that an end-on (diketiminate)copper(II) superoxide isomer is only ∼5 kcal mol^{-1} less stable than the side-on product[6b] and that decreasing the electron-donating power of the diketiminate could decrease this energy gap and potentially enable isolation of the end-on copper(II) superoxide form.[8] In an initial experimental test of this hypothesis, copper(I) complexes of **1** and **2** featuring CF_3 replacements for the backbone methyl groups were prepared and reacted with O_2. While (**1**)Cu(NCMe) yielded a side-on copper(III) peroxide, no intermediate was observed for (**2**)Cu(NCMe), consistent with calculations showing that the oxygenation is endergonic in this case.[8] It was therefore concluded that, in order for a bidentate ligand to support end-on copper(II) superoxide formation, a balance must be achieved such that the ligand electronics favor this isomer over the side-on copper(III) peroxide variant, but which also results in favorable thermodynamics for O_2 binding.[8]

The research described herein was undertaken to further explore bidentate ligand electronic and structural effects on the Cu^I/O_2 reactivity. We hypothesized that while not observed, a 1:1 Cu/O_2 adduct from oxygenation of (**2**)Cu(NCMe) might be present at a low equilibrium concentration. To test this idea, we sought to trap a similar 1:1 Cu/O_2 adduct supported by **4**,[9] which we proposed would have electronic/redox properties similar to those of **2** but by virtue of its decreased steric bulk could enable the irreversible formation of a bis(μ-oxo)dicopper complex like that known for **3**.[5b] In parallel, we turned to nitroformazan **5** as a potential supporting ligand analogous to the diketiminates[10,11] but with unique properties, including lower electron-donating capabilities and accessibility of a verdazyl radical form.[12,13] Herein we report the synthesis and characterization of copper(I) complexes of electron-poor ligands **4** and **5** (relative to diketiminates like **3**), along with the results of their low-temperature oxygenation reactions. Combined spectroscopic and theoretical studies support the formation of bis(μ-oxo)dicopper complexes in both cases, implicating the intermediacy of 1:1 Cu/O_2 adducts as transient intermediates. As a result of the unique characteristics of **5**, its bis(μ-oxo)dicopper complex exhibits unusual properties and decays via the intermediacy of a novel ligand-centered radical species.

Experimental Section

General Considerations. All solvents and reagents were obtained from commercial sources and used as received unless otherwise noted. The solvents tetrahydrofuran (THF), pentane, and Et_2O were dried over sodium/benzophenone and distilled under vacuum or passed through solvent purification columns (Glass Contour, Laguna, CA). Acetonitrile (CH_3CN) was dried over CaH_2 and distilled under vacuum prior to use. [Cu_4Mes_4] (Mes = mesityl)[14] and the protonated forms of **4**[9] and **5**[10] were prepared according to published procedures. All metal complexes were prepared and stored in a Vacuum Atmospheres inert-atmosphere glovebox under a dry N_2 atmosphere or were manipulated using standard inert-atmosphere vacuum and Schlenk techniques. NMR spectra were recorded on either Varian VI-300 or VI-500 spectrometers at room temperature. Variable low-temperature NMR spectra were recorded on a Varian VI-300 spectrometer. Chemical shifts (δ) for ^1H (300 MHz) and ^{13}C (75 MHz) NMR spectra were referenced to residual solvent signal. UV−vis spectra were recorded on an HP8453 (190−1100 nm) diode-array spectrophotometer. Low-temperature spectra were acquired through the use of a Unisoku low-temperature UV−vis cell holder. When necessary, UV−vis spectra were corrected for drifting baselines due to minimal frosting of the UV cells caused by the low-temperature device. This was achieved by subtracting the average of a region with no absorbance (i.e., baseline, typically 950−1000 nm) from the entire spectrum. X-band electron paramagnetic resonance (EPR) spectra were recorded on a Bruker E-500 spectrometer with an Oxford Instruments EPR-10 liquid-helium cryostat (4−20 K, 9.61 GHz). Resonance Raman (rR) spectra were recorded on an Acton 506 spectrometer using a Princeton Instruments LN/CCD-11100-PB/

(5) (a) Spencer, D. J. E.; Aboelella, N. W.; Reynolds, A. M.; Holland, P. L.; Tolman, W. B. *J. Am. Chem. Soc.* **2002**, *124*, 2108–2809. (b) Spencer, D. J. E.; Reynolds, A. M.; Holland, P. L.; Jazdzewski, B. A.; Duboc-Toia, C.; Pape, L. L.; Yokota, S.; Tachi, Y.; Itoh, S.; Tolman, W. B. *Inorg. Chem.* **2002**, *41*, 6307–6321.
(6) (a) Aboelella, N. W.; Lewis, E. A.; Reynolds, A. M.; Brennessel, W. W.; Cramer, C. J.; Tolman, W. B. *J. Am. Chem. Soc.* **2002**, *124*, 10660–10661. (b) Aboelella, N. W.; Kryatov, S. V.; Gherman, B. F.; Brennessel, W. W.; Victor, G.; Young, J.; Sarangi, R.; Rybak-Akimova, E. V.; Hodgson, K. O.; Hedman, B.; Solomon, E. I.; Cramer, C. J.; Tolman, W. B. *J. Am. Chem. Soc.* **2004**, *126*, 16896–16911.
(7) (a) Sarangi, R.; Aboelella, N.; Fujisawa, K.; Tolman, W. B.; Hedman, B.; Hodgson, K. O.; Solomon, E. I. *J. Am. Chem. Soc.* **2006**, *128*, 8286–8296. (b) Gherman, B. F.; Tolman, W. B.; Cramer, C. J. *J. Comput. Chem.* **2006**, *27*, 1950–1961.
(8) Hill, L. M. R.; Gherman, B. F.; Aboelella, N. W.; Cramer, C. J.; Tolman, W. B. *Dalton Trans.* **2006**, 4944–4953.
(9) Carey, D. T.; Cope-Eatough, E. K.; Vilaplana-Mafé, E.; Mair, F. S.; Pritchard, R. G.; Warren, J. E.; Woods, R. J. *Dalton Trans.* **2003**, 1083–1093.
(10) Gilroy, J. B.; Otieno, P. O.; Ferguson, M. J.; McDonald, R.; Hicks, R. G. *Inorg. Chem.* **2008**, *47*, 1279–1286.
(11) Gilroy, J. B.; Patrick, B. O.; McDonald, R.; Hicks, R. G. *Inorg. Chem.* **2008**, *47*, 1287–1294.
(12) Koivisto, B. D.; Hicks, R. G. *Coord. Chem. Rev.* **2005**, *249*, 2612–2630.
(13) Gilroy, J. B.; Ferguson, M. J.; McDonald, R.; Patrick, B. O.; Hicks, R. G. *Chem. Commun.* **2007**, 126.
(14) Tsuda, T.; Yazawa, T.; Watanabe, K.; Fujii, T.; Saegusa, T. *J. Org. Chem.* **1981**, *46*, 192–194.

UVAR detector and a ST-1385 controller interfaced with *Winspec* software. The spectra were obtained at −196 °C using a backscattering geometry. Excitation at 457.9 and 514.5 nm was provided by a Spectra Physics BeamLok 2065-7S argon laser. Raman shifts were externally referenced to liquid indene. Elemental analyses were performed by Robertson Microlit Laboratory. Electrospray ionization mass spectrometry spectra were recorded on a Bruker BioTOF II instrument. IR spectra were obtained using a ThermoNicolet Avatar 370 FT-IR equipped with an attenuated total reflectance attachment, using a CaF_2 solution cell (International Crystal Laboratories). Cyclic voltammograms were recorded using platinum working and auxiliary electrodes, a silver wire/$AgNO_3$ (10 mM in CH_3CN) reference electrode, and a BAS Epsilon potentiostat connected to a 22 mL cell in an inert-atmosphere glovebox. Experiments were performed using analyte concentrations of 1 mM in THF with 0.3 M tetrabutylammonium hexafluorophosphate, $TBAPF_6$ (sample volumes of ∼5 mL), at room temperature. The ferrocene/ferrocenium (Fc/Fc^+) couple was recorded for reference.

Theory. All molecular structures were fully optimized using the generalized gradient approximation (GGA) density functional (*m*PW) that combines the exchange functional of Perdew,[15] as modified by Adamo and Barone,[16] with the correlation functional of Perdew and Wang.[17] Atomic orbital basis functions were taken for copper from the Stuttgart effective core potential and basis set,[18] including two f functions having exponents 5.208 and 1.315, and for all other atoms from the 6-31G(d) basis set.[19] Resolution of the identity density fitting was employed in all cases, and restricted singlet Kohn−Sham wave functions were determined in every instance to be stable relative to unrestricted alternatives [restricted to unrestricted singlet instabilities have been demonstrated in other bis(μ-oxo) species[20]]. Analytical vibrational frequencies were computed for all stationary points in order to confirm their nature as minima or transition-state structures and for comparison to IR or rR spectra, as appropriate.[21] For select molecules, the first 90 vertical electronic excitation energies were computed at the time-dependent (TD-)DFT level[22] using the hybrid GGA B3LYP[23−26] functional and a polarized valence double-ζ basis set[27,28] on all atoms. Electronic structure calculations were accomplished with the *Gaussian 03*[29] and *Turbomole*[27] program suites.

(4)Cu(CH_3CN). In an inert atmosphere, to a solution of the ligand precursor H(**4**) (100 mg, 0.24 mmol) in CH_3CN (5 mL) was added [Cu_4Mes_4] (44 mg, 0.06 mmol). After the reaction mixture was vigorously stirred overnight, it was filtered through a plug of Celite to remove any insoluble residue. The solvent was removed from the filtrate in vacuo to give a brown residue. The product was isolated in analytically pure form by allowing a concentrated solution of the residue in CH_3CN to stand for 3 days at −20 °C. The resulting orange crystals were separated from the mother liquor, washed with cold pentane (∼5 mL), and dried in vacuo (93 mg, 75%). ^{1}H NMR (300 MHz, benzene-d_6): δ 6.99 (d, J = 7.5 Hz, 4H), 6.91 (t, J = 7.5 Hz, 2H), 6.11 (s, 1H), 2.11 (s, 12H), 0.28 (s, 3H). ^{13}C{^{1}H} NMR (75.0 MHz, benzene-d_6): δ 152.40, 148.56, 143.57, 130.33, 124.39, 123.23, 119.43, 83.77, 19.19, 0.27. UV−vis [λ_{max}, nm (ϵ, M^{-1} cm^{-1}) in THF]: 280 (18 900), 381 (16 600), 500 (460). Anal. Calcd for $C_{23}H_{22}CuF_6N_3$: C, 53.33; H, 4.28; N, 8.11. Found: C, 53.56; H, 4.08; N, 8.08.

(5)Cu(CH_3CN). This compound was synthesized following the same procedure as described above, except using H(**5**) as the starting material and crystallizing the product by slow diffusion of pentane into a concentrated THF solution at −20 °C (99 mg, 80%). ^{1}H NMR (300 MHz, benzene-d_6): δ 7.15 (m, 6H), 3.40 (septet, J = 6.9 Hz, 4H), 1.24 (d, J = 6.9 Hz, 24H), 0.17 (s, 3H). ^{13}C{^{1}H} NMR (75.0 MHz, benzene-d_6): δ 151.46, 141.24, 127.85, 124.29, 29.06, 25.02, 23.71, 0.27. UV−vis [λ_{max}, nm (ϵ, M^{-1} cm^{-1}) in THF]: 287 (11 700), 352 (9480), 410 (10 500), 650 (380). Anal. Calcd for $C_{27}H_{37}CuN_6O_2$: C, 59.92; H, 6.89; N, 15.53. Found: C, 59.75; H, 6.91; N, 15.74.

LCu(CO) (L = 3, 4, or 5). General Procedure. The complex LCu(CH_3CN) (L = **3**, **4**, or **5**; 37 μmol) was dissolved in benzene-d_6 (0.8 mL) in a screw-capped NMR tube. Carbon monoxide (CO) was gently bubbled through the solution for 20 min at ambient temperature, during which time the color changed to gold for L = **3** and **4** and dark red for L = **5**. The CO adducts were immediately characterized by ^{1}H and ^{13}C NMR spectroscopy. For IR characterization, the complex LCu(CH_3CN) (37 μmol) was dissolved in THF (2 mL) in a 10 mL Schlenk tube and stirred with CO bubbling at ambient pressure for 2 h, during which time the solvents evaporated. Approximately half of the dried solid (golden to dark red) was dissolved in THF (0.4 mL), and the IR spectrum was recorded immediately. (**3**)Cu(CO). ^{1}H NMR (300 MHz, benzene-d_6): δ 7.05 (d, J = 7.5 Hz, 4H), 6.94 (t, J = 7.5 Hz, 2H), 4.92 (s, 1H), 2.21 (s, 12H), 1.62 (s, 6H). ^{13}C{^{1}H} NMR (75.0 MHz, benzene-d_6): δ 164.25, 152.56, 130.40, 128.98, 124.24, 95.59, 22.49, 12.29. FT-IR (THF): 2071 cm^{-1} (ν_{CO}). (**4**)Cu(CO). ^{1}H NMR (300 MHz, benzene-d_6): δ 6.96−6.86 (m, 6H), 6.16 (s, 1H), 2.13 (s, 12H). ^{13}C{^{1}H} NMR (75.0 MHz, benzene-d_6): δ 153.65, 149.30, 129.92, 125.48, 122.89, 119.09, 85.67, 19.12. FT-IR (THF): 2100 cm^{-1} (ν_{CO}). (**5**)Cu(CO). ^{1}H NMR (300 MHz, benzene-d_6): δ 7.24−7.08 (m, 6H), 3.24 (sept, J = 6.9 Hz, 4H), 1.20 (s, 24H).

(15) Perdew, J. P. Unified Theory of Exchange and Correlation Beyond the Local Density Approximation. In *Electronic Structure of Solids '91*; Ziesche, P., Eschrig, H., Eds.; Akademie Verlag: Berlin, 1991; pp 11−20.
(16) Adamo, C.; Barone, V. *J. Chem. Phys.* **1998**, *108*, 664–675.
(17) Perdew, J.; Wang, Y. *Phys. Rev. B* **1992**, *45*, 13244–13249.
(18) Dolg, M.; Wedig, U.; Stoll, H.; Preuss, H. *J. Chem. Phys.* **1987**, *86*, 866–872.
(19) Hehre, W. J.; Radom, L.; Schleyer, P. v. R.; Pople, J. A. *Ab Initio Molecular Orbital Theory*; Wiley: New York, 1986.
(20) Gherman, B. F.; Cramer, C. J. *Coord. Chem. Rev.* **2009**, *253*, 723–753.
(21) Cramer, C. J. *Essentials of Computational Chemistry: Theories and Models*, 2nd ed.; John Wiley & Sons: Chichester, U.K., 2004.
(22) Bauernschmitt, R.; Ahlrichs, R. *Chem. Phys. Lett.* **1996**, *256*, 454–464.
(23) Becke, A. D. *Phys. Rev. A* **1988**, *38*, 3098–3100.
(24) Becke, A. D. *J. Chem. Phys.* **1993**, *98*, 5648–5652.
(25) Lee, C.; Yang, W.; Parr, R. G. *Phys. Rev. B* **1988**, *37*, 785–789.
(26) Stephens, P. J.; Devlin, F. J.; Chabalowski, C. F.; Frisch, M. J. *J. Phys. Chem.* **1994**, *98*, 11623–11627.
(27) Ahlrichs, R.; Bär, M.; Häser, M.; Horn, H.; Kölmel, C. *Chem. Phys. Lett.* **1989**, *162*, 165–169.
(28) Schafer, A.; Horn, H.; Ahlrichs, R. *J. Chem. Phys.* **1992**, *97*, 2571–2577.
(29) Frisch, M. J.; Trucks, G. W.; Schlegel, H. B.; Scuseria, G. E.; Robb, M. A.; Cheeseman, J. R.; Montgomery, J. A.; Vreven, T.; Kudin, K. N.; Burant, J. C.; Millam, J. M.; Iyengar, S. S.; Tomasi, J.; Barone, V.; Mennucci, B.; Cossi, M.; Scalmani, G.; Rega, N.; Petersson, G. A.; Nakatsuji, H.; Hada, M.; Ehara, M.; Toyota, K.; Fukuda, R.; Hasegawa, J.; Ishida, M.; Nakajima, T.; Honda, Y.; Kitao, O.; Nakai, H.; Klene, M.; Li, X.; Knox, J. E.; Hratchian, H. P.; Cross, J. B.; Adamo, C.; Jaramillo, J.; Gomperts, R.; Stratmann, R. E.; Yazyev, O.; Austin, A. J.; Cammi, R.; Pomelli, C.; Ochterski, J. W.; Ayala, P. Y.; Morokuma, K.; Voth, G. A.; Salvador, P.; Dannenberg, J. J.; Zakrzewski, V. G.; Dapprich, S.; Daniels, A. D.; Strain, M. C.; Farkas, O.; Malick, D. K.; Rabuck, A. D.; Raghavachari, K.; Foresman, J. B.; Ortiz, J. V.; Cui, Q.; Baboul, A. G.; Clifford, S.; Cioslowski, J.; Stefanov, B. B.; Liu, G.; Liashenko, A.; Piskorz, P.; Komaromi, I.; Martin, R. L.; Fox, D. J.; Keith, T.; Al-Laham, M. A.; Peng, C. Y.; Nanayakkara, A.; Challacombe, M.; Gill, P. M. W.; Johnson, B.; Chen, W.; Wong, M. W.; Gonzalez, C.; Pople, J. A. *Gaussian 03*, Revision D.02; Gaussian, Inc.: Wallingford, CT, 2004.
(30) Battino, R. *Oxygen and Ozone*; Battino, R., Ed.; Pergamon Press: New York, 1981; Vol. *7*.

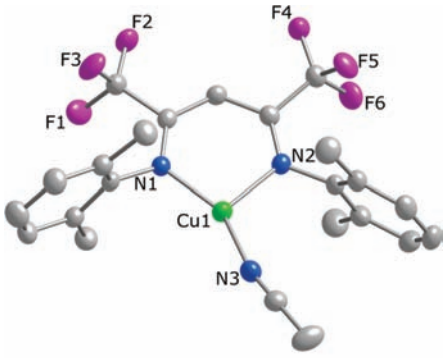

Figure 2. Representation of the X-ray structure of (**4**)Cu(CH_3CN) with all non-H atoms shown as 50% thermal ellipsoids. Selected interatomic distances (Å) and angles (deg): Cu1−N3, 1.871(2); Cu1−N1, 1.902(2); Cu1−N2, 1.998(2); N3−Cu1−N1, 148.46(9); N3−Cu1−N2, 111.57(9); N1−Cu1−N2, 99.01(9).

$^{13}C\{^1H\}$ NMR (75.0 MHz, benzene-d_6): δ 151.62, 151.34, 141.30, 129.92, 124.52, 29.09, 25.40, 23.43. FT-IR (THF): 2092 cm^{-1} (ν_{CO}).

$L_2Cu_2(OH)_2$ (L = 4 or 5). Solutions of LCu(CH_3CN) (L = **4** or **5**) in THF (∼50 mg in 10 mL) were oxygenated by bubbling of O_2 at ambient temperature for ∼1 min. For L = **4**, the resulting red-brown solution was layered with ∼10 mL pentane and allowed to stand at −20 °C. Red single crystals formed after several days and were either mounted for analysis by X-ray crystallography or collected by decanting the mother liquor, washing with cold pentane, and drying in vacuo (19 mg, 40%). Anal. Calcd for $C_{42}H_{40}Cu_2F_{12}N_4O_2$: C, 51.06; H, 4.08; N, 5.67. Found: C, 51.76; H, 4.30; N, 5.27. Red single crystals of the product of the reaction of (**5**)Cu(CH_3CN) were obtained by slow evaporation of the red-brown reaction solution and were isolated similarly (21 mg, 44%). Anal. Calcd for $C_{50}H_{70}Cu_2N_{10}O_6$: C, 58.06; H, 6.82; N, 13.54. Found: C, 57.67; H, 6.91; N, 13.28.

Low-Temperature Oxygenations of LCu(CH_3CN) (L = 4 or 5). (a) UV−Vis Spectroscopy. An anaerobically prepared THF solution of (**4**)Cu(CH_3CN) (0.2 mM) or (**5**)Cu(CH_3CN) (0.1 mM) in a septum-sealed quartz cuvette was cooled to −80 °C, and a dry stream of O_2 was bubbled through the solution for ∼20 min or ∼100 s, respectively. The spectroscopic changes are shown in Figure 5. The final spectrum was not perturbed by removal of excess O_2 from the solution by an argon purge. For L = **5**, after bubbling argon for 30 min through the solution to remove the remaining unreacted O_2, the solution was warmed above −50 °C, resulting in the disappearance of the band at 525 nm and the growth of a new sharp feature at 742 nm, which subsequently decayed (Figure 8). The same intermediate spectrum was also generated by directly oxygenating (**5**)Cu(CH_3CN) above −50 °C.

(b) rR Spectroscopy. An argon-filled Schlenk flask or NMR tube was charged with 1 mL of a THF solution of LCu(CH_3CN) (L = **4** or **5**; 40 mM for L = **4** and 10 mM for L = **5**) by syringe and cooled to −80 °C by submersion in an acetone/dry ice bath while maintaining an argon purge. Dry O_2 was bubbled through the solution (30 min for L = **4** and 10 min for L = **5**). Samples were frozen either in a copper cup attached to a liquid-N_2-cooled coldfinger (L = **4**) or by immersion in the NMR tube in liquid N_2 (L = **5**). For reactions with $^{18}O_2$, a 10 mL Schlenk tube charged with 1 mL of a THF solution of LCu(CH_3CN) (L = **4** or **5**) was frozen in liquid N_2 and ∼10 mL of $^{18}O_2$ was vacuum-transferred to the flask. The resulting mixture was warmed to −80 °C by submersion in an acetone/dry ice bath and stirred for 3 h to ensure complete reaction. Samples for analysis by rR spectroscopy were prepared by transferring a sample of the reaction mixture either to a copper cup or to a precooled NMR tube (−80 °C) followed by immersion in liquid N_2.

(c) EPR Spectroscopy. A 10 mL Schlenk flask was charged with a THF solution of LCu(CH_3CN) (L = **4** or **5**) (2 mM) and was cooled to −80 °C in an acetone/dry ice bath. Dry O_2 was bubbled through the solution (30 min for L = **4** and 10 min for L = **5**), and the resulting solution was transferred via a precooled syringe to a precooled (−80 °C) EPR tube, which was immersed in liquid N_2 for subsequent analysis by EPR spectroscopy. Also, a quartz cuvette was charged with a THF solution of (**5**)Cu(CH_3CN) (2 mM), cooled to −30 °C, and oxygenated by bubbling dry O_2 with monitoring of the feature at 742 nm by UV−vis spectroscopy. Aliquots of the solution were rapidly transferred at various time points via a syringe to a precooled (−80 °C) EPR tube, which was immersed in liquid N_2 for subsequent analysis by EPR spectroscopy.

(d) Spectrophotometric O_2 Titrations. A 1 mL sample of a stock solution of LCu(CH_3CN) (L = **4** or **5**) in THF (1.0 mM for **4** and 0.5 mM for **5**) was placed in a 0.2-cm-path-length UV−vis cuvette and cooled to −80 °C, and the headspace was evacuated. Spectra were taken before and after cooling to ensure that no sample degradation had occurred. An O_2-saturated THF solution (10 mM) was prepared by bubbling dry O_2 gas through argon-saturated THF in a 10 mL Schlenk tube at 25 °C for 15 min.[29] Using a graduated gastight syringe, portions of the 10 mM O_2-saturated THF solution (10, 20, 30, 40, 50, 75, 100, 150, and 200 μL) were injected into the cuvette, where it was left to equilibrate with stirring. The progress of oxygenation was followed by monitoring of the absorption band at 470 nm (**4**) or 524 nm (**5**) in the UV−vis spectrum until no further increase in absorbance was observed. The Cu/O_2 stoichiometry was calculated from two (L = **4**) or three (L = **5**) replicate runs.

Results and Discussion

Copper(I) Complexes. The complexes LCu(CH_3CN) (L = **4** or **5**) were prepared by the reaction of [Cu_4Mes_4] with the protonated forms of **4** or **5** in CH_3CN and were characterized by NMR and UV−vis spectroscopy, elemental analysis, cyclic voltammetry, and X-ray crystallography (Figures 2and S1 in the Supporting Information). Both compounds exhibit three-coordinate Cu^I ions and gross structural features similar to other known copper(I) complexes of diketiminate ligands, although the structure for (**5**)Cu(CH_3CN) suffers from disorder problems that preclude more detailed analysis of interatomic distances and angles. In (**4**)Cu(CH_3CN), the Cu^I ion adopts a geometry close to T-shaped, with divergent Cu−N(diketiminate) distances of 1.902(2) and 1.998(2) Å. The C(backbone)−N−C(aryl) angles in (**4**)Cu(CH_3CN) (122−125°) are wider than those in the copper complex of the analogue **3** (116−120°),[31,32] indicative of steric pressure from the CF_3 groups that places the aryl substituents closer to the bound metal ion. The effect has important implications in reactivity studies (see below), although even wider angles are observed for systems with *tert*-butyl backbone substituents (128−129°).[6,33]

(31) Dai, X.; Warren, T. H. *Chem. Commun.* **2001**, 1998–1999.
(32) York, J. T.; Young, V. G.; Tolman, W. B. *Inorg. Chem.* **2006**, *45*, 4191–4198.
(33) Vela, J.; Vaddadi, S.; Cundari, T. R.; Smith, J. M.; Gregory, E. A.; Lachicotte, R. J.; Flaschenriem, C. J.; Holland, P. L. *Organometallics* **2004**, *23*, 5226–5239.

Table 1. Properties of Copper(I) Complexes of Diketiminate and Formazan Ligands

ligand	$E_{1/2}$ (mV)[a]	ν(CO) exptl (cm^{-1})[b]	ν(CO) calcd (cm^{-1})[c]	ref
1	110	2083	2074	8 (exptl), this work (calcd)
2	411	2097	2082	8 (exptl), this work (calcd)
3	*d*	2071	2070	this work
4	134	2100	2088	this work
5	103	2092	2084	this work

[a] Measured for LCu(CH_3CN) in THF with $TBAPF_6$ (0.3 M) vs Fc/Fc^+. [b] Measured for the copper(I) carbonyl complex in THF. [c] Computed values for copper(I) carbonyl complexes at the *m*PW level after correction by 19 cm^{-1}, which is the difference between *m*PW and experiment for CO gas. [d] Value reported previously but under different conditions than those used in this work (CH_3CN solvent), and this fact along with previously noted complications with reproducibility for this complex makes comparison of the ν(CO) values more useful for drawing comparisons among the complexes listed.[5b]

In order to probe the effects of **4** and **5** on the redox properties of their copper(I) compounds, we performed electrochemistry experiments and prepared CO adducts for characterization by FT-IR spectroscopy. Cyclic voltammograms (Figure S2 in the Supporting Information) of THF solutions of LCu(CH_3CN) (L = **4** or **5**) with $TBAPF_6$ (0.3 M) exhibited pseudoreversible waves with $E_{1/2}$ values of +134 mV (**4**) and +103 mV (**5**) versus Fc/Fc^+ ($\Delta E_{p,c}$ = 118 and 112 mV, respectively, at a scan rate of 20 mV s^{-1}). These electrochemical results, as well as ν(CO) values for their CO adducts, are compared to data for related compounds obtained under similar conditions in Table 1. As noted in previous work,[8] replacement of the backbone methyl group in **1** by a CF_3 group to yield **2** results in a 14 cm^{-1} increase in the ν(CO) value for LCuCO and a ~300 mV increase in the $E_{1/2}$ value for LCu(CH_3CN), consistent with **2** being a poorer electron donor that yields a more Lewis acidic and less readily oxidized copper(I) center. A similar effect is evident from the ν(CO) values for the complexes of **3** and **4**. Like **2**, **4** has two backbone CF_3 groups, and it exhibits a similar ν(CO) value for its copper(I) carbonyl complex, which implies analogous electron-donating properties for these two ligands, which only differ with respect to their aryl substituents (Me vs iPr). Gas-phase theoretical calculations of the CO stretching frequencies are in good agreement with the measured values (see Table 1), indicating the degree to which they reflect ligand effects on the molecular electronic structure.

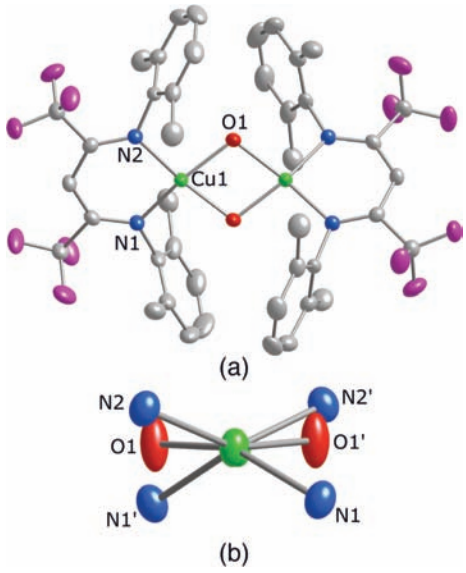

Figure 3. (a) Representation of the X-ray structure of $(\mathbf{4})_2Cu_2(OH)_2$ with all non-H atoms shown as 50% thermal ellipsoids. (b) View down the Cu−Cu vector; C and F atoms are not shown for clarity. Selected interatomic distances (Å) and angles (deg): Cu1−O1′, 1.9105(18); Cu1−O1, 1.9121(18); Cu1−N2, 1.940(2); Cu1−N1, 1.943(2); Cu1−Cu1′, 3.0195(6); O1′−Cu1−O1, 75.44(9); O1′−Cu1−N2, 159.07(9); O1−Cu1−N2, 97.82(8); O1′−Cu1−N1, 97.93(8); O1−Cu1−N1, 157.40(9); N2−Cu1−N1, 95.28(8).

However, in apparent contradiction to the conclusions based on the ν(CO) values, the $E_{1/2}$ value for (**4**)Cu(CH_3CN) is 277 mV lower than that for the complex with **2**. We speculate that this difference results from two possible effects of the differing aryl substituents of **2** and **4**. One is the greater hydrophobicity of the diisopropylphenyl groups in **2** compared to the dimethylphenyl groups in **4**, which for **2** would result in relative destabilization of the more highly charged copper(II) state and a greater $E_{1/2}$. Another effect is primarily steric; the copper(I) complex of more hindered **2** likely remains three-coordinate upon oxidation, whereas the smaller steric profile for **4** could enable binding of two (or more) solvent molecules upon oxidation of its copper(I) complex, resulting in enhanced stability for the copper(II) state and a smaller $E_{1/2}$. Because of these hydrophobic and steric influences, we view the ν(CO) values as more reliable indicators of the relative electron density at the metal center, a conclusion similar to that reached in previous studies of other diketiminate−copper complexes.[5b] Thus, on the basis of the ν(CO) data, nitroformazan **5** and diketiminates **2** and **4** have similar electron-donating characteristics.

Oxygenation of Copper(I) Complexes. (a) Room Temperature Reactions: Formation of Bis(hydroxo)dicopper Complexes. Treatment of LCu(CH_3CN) (L = **4** or **5**) in THF with O_2 at ambient temperature rapidly (<1 min) yielded red-brown solutions, from which $L_2Cu_2(\mu\text{-}OH)_2$ could be isolated as crystalline solids in modest yields (40−44%). The products were identified by elemental analysis and X-ray crystallography (Figures 3 and 4). The structure of $(\mathbf{4})_2Cu_2(OH)_2$ features a separation of 3.0195(6) Å between Cu^{II} ions that adopt distorted square-planar geometries characterized by a τ_4 value of 0.31, where τ_4 = 1.00 is associated with perfect tetrahedral and τ_4 = 0 with perfect square-planar coordination geometries.[34] Steric repulsions between the aryl groups are apparently minimized by twisting of the ligand planes with respect to each other, reflected by a dihedral angle between the N atoms (N1−Cu1−N2/N1′−Cu1′−N2′) of 56.31° (Figure 3b). Similar twisting has been observed previously in a bis(μ-chloro)dicopper(II) complex supported by a diketiminate ligand with the same dimethylphenyl groups as in **3**.[5a] Similar to the structure of (**4**)Cu(CH_3CN), the CF_3 groups cause canting of the aryl rings toward the coordinated Cu ion, as reflected by C(backbone)−N−C(aryl) angles of almost 123°.

(34) Yang, L.; Powell, D.; Houser, R. *Dalton Trans.* **2007**, 955–964.

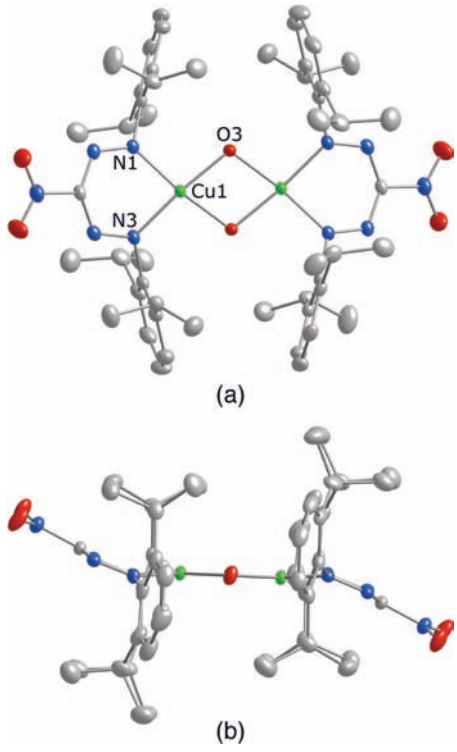

Figure 4. (a) Representation of the X-ray structure of $(\mathbf{5})_2Cu_2(OH)_2$ with all non-H atoms shown as 50% thermal ellipsoids. (b) Alternate view by rotating part (a) by 90°. Selected interatomic distances (Å) and angles (deg): Cu1−O3, 1.9179(13); Cu1−O3′, 1.9294(13); Cu1−N1, 1.9519(15); Cu1−N3, 1.9646(15); Cu1−Cu1′, 3.0278(5); O3−Cu1′, 1.9294(13); O3−Cu1−O3′, 76.19(6); O3−Cu1−N1, 172.51(6); O3′−Cu1−N1, 96.95(6); O3−Cu1−N3, 98.50(6); O3′−Cu1−N3, 173.05(6); N1−Cu1−N3, 88.09(6); N3−Cu1−Cu1′, 136.57(5); Cu1−O3−Cu1′, 103.81(6).

Complex $(\mathbf{5})_2Cu_2(OH)_2$ also features a planar bis(hydroxo)-dicopper(II) core, with a Cu−Cu distance of 3.0278(5) Å (Figure 4). Interligand interactions are minimized in this case by canting of the ligands away from the plane of the core by ∼27° (Figure 4b). Also, the lack of substituents on the N atom adjacent to the ligated N atom results in small N−N−C(aryl) angles of ∼112° and a decreased steric profile for the formazan, notwithstanding the presence of the isopropyl substituents on the aryl rings.[5b] The formazan−copper metallocycle appears as a boatlike conformation because of displacement of the central C atom and the Cu atom away from the plane defined by the formazan N atoms. Similar conformational properties have been seen for related formazan complexes.[11,13,35]

(b) Low-Temperature Reactions: Identification of Intermediates. Oxygenation of LCu(CH_3CN) (L = **4** or **5**) at −80 °C in THF resulted in the growth of new features in the UV−vis spectra that were unperturbed upon removal of excess O_2 but which bleached upon warming (Figure 5). New features below 400 nm (**4**) (not shown) or 500 nm (**5**) are likely to arise in large part from ligand-based $\pi-\pi^*$ transitions, and a weak band at 780 nm ($\varepsilon = 200$ M^{-1} cm^{-1}) was also observed for the system supported by **4**. Most importantly, oxygenation resulted in intense new bands at 470 nm ($\epsilon \sim 15\,000$ M^{-1} cm^{-1}; **4**) or 525 nm ($\epsilon \sim 23\,000$ M^{-1} cm^{-1}; **5**) that are suggestive of charge-transfer (CT) transitions associated with bis(μ-oxo)dicopper cores.[2a,b,36] Spectrophotometric titration results confirmed the requisite 2:1 Cu/O_2 stoichiometry (insets to plots in Figure 5). However, the UV−vis bands are shifted to longer wavelengths relative to typical $[Cu_2(\mu\text{-}O)_2]^{2+}$ core electronic transitions that occur in the ranges 300−330 nm ($\epsilon \sim 10\,000-20\,000$ M^{-1} cm^{-1}) and 400−450 nm ($\epsilon \sim 10\,000-30\,000$ M^{-1} cm^{-1}). The 525 nm band for the complex supported by **5** is a particularly notable outlier at energy significantly different from that of typical bis(μ-oxo)dicopper core transitions. A low-energy feature at 550 nm with an extinction much lower than what we observe (1300 M^{-1} cm^{-1}) was reported for a bis(μ-oxo)dicopper complex supported by a guanidine ligand and assigned as a guanidine → $[Cu_2(\mu\text{-}O)_2]^{2+}$ CT transition.[37]

To provide further insights, we performed rR spectroscopy experiments on samples prepared using $^{16}O_2$ or $^{18}O_2$ with excitation wavelengths of 457.9 nm (**4**) or 514.5 nm (**5**). The spectrum for the oxygenated product of (**4**)Cu(CH_3CN) (Figure 6a) contains two peaks at 598 and 610 cm^{-1} that are replaced by a single peak at 566 cm^{-1} upon ^{18}O labeling. This pattern has been seen previously for bis(μ-oxo)dicopper complexes[36,38] and is usually attributed to a symmetric Cu_2O_2 core vibration that appears as a Fermi doublet with $^{16}O_2$ but converts to a single peak with $^{18}O_2$. For the case of the reaction with (**5**)Cu(CH_3CN) (Figure 6b), a peak at 581 cm^{-1} appears to shift to 558 cm^{-1} upon use of $^{18}O_2$, although an overlapping additional peak at 581 cm^{-1} complicates the analysis. As shown in the inset to Figure 6b, frequency-doubled overtone peaks are observed at 1160 cm^{-1} ($^{16}O_2$) and 1112 cm^{-1} ($^{18}O_2$). The combined data for both cases **4** and **5** are consistent with the assignment of the 470 and 525 nm transitions, respectively, as CT transitions involving bis(μ-oxo)dicopper cores. Also consistent with these formulations, the intermediates are EPR-silent (X-band, 4 K).

Computational Assessment of Oxygenation Reactions. DFT calculations at the *m*PW level of theory were carried out to gain additional insight into structural and spectroscopic characteristics of the bis(μ-oxo)dicopper complexes of **4** and **5** (the full calculated geometries of all species are available as Supporting Information; the structure of **5** is shown in Figure S5). For **4**, two different geometric isomers are predicted to be minima; the lower energy isomer belongs to the D_2 point group and has a core structure resembling that of the bis(hydroxo)dicopper complex shown in Figure 3, including an N−Cu−Cu−N torsion angle of 47.7°. The other structure belongs to the C_{2h} point group

(35) Gilroy, J. B.; Ferguson, M. J.; McDonald, R.; Hicks, R. G. *Inorg. Chim. Acta* **2008**, *361*, 3388–3393.

(36) Henson, M. J.; Mukherjee, P.; Root, D. E.; Stack, T. D. P.; Solomon, E. I. *J. Am. Chem. Soc.* **1999**, *121*, 10332–10345.

(37) Herres-Pawlis, S.; Verma, P.; Haase, R.; Kang, P.; Lyons, C. T.; Wasinger, E. C.; Flörke, U.; Henkel, G.; Stack, T. D. P. *J. Am. Chem. Soc.* **2009**, ASAP; doi: 10.1021/ja807809x.

(38) Holland, P. L.; Cramer, C. J.; Wilkinson, E. C.; Mahapatra, S.; Rodgers, K. R.; Itoh, S.; Taki, M.; Fukuzumi, S.; Que, L., Jr.; Tolman, W. B. *J. Am. Chem. Soc.* **2000**, *122*, 792–802.

(39) Theory also offers support for the possible experimental occurrence of Fermi resonances in these cases, insofar as there are many normal modes predicted to have fundamental frequencies near half of the breathing-mode frequencies, so that overtones of the former might be expected to couple with the latter.

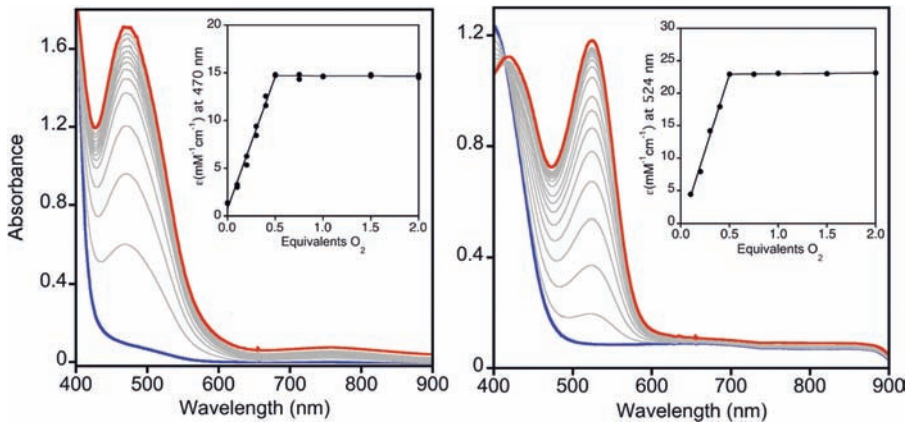

Figure 5. UV−vis changes accompanying oxygenation of (left) (**4**)Cu(CH_3CN) and (right) (**5**)Cu(CH_3CN) at −80 °C in THF, using starting concentrations of 0.2 or 0.1 mM, respectively. The initial and final spectra are in blue and red, respectively. The insets show the results of spectrophotometric titrations of the complexes with O_2 as linear fits to (left) data for two replicate runs or (right) average data from three replicate runs.

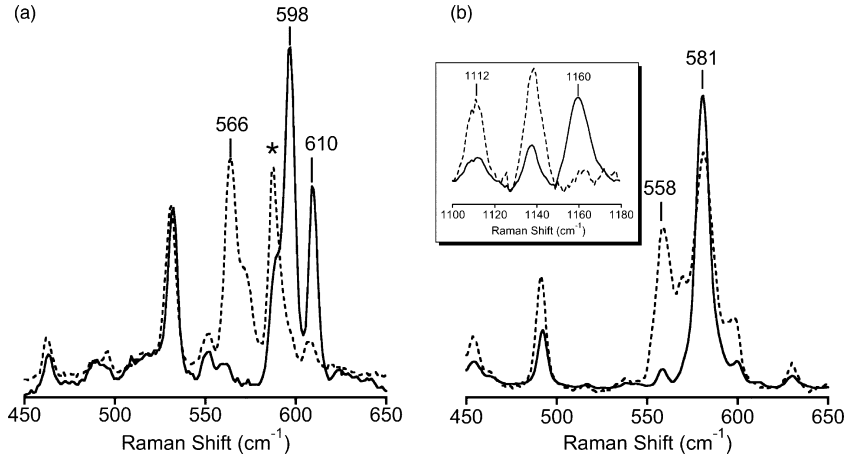

Figure 6. rR spectra of the frozen solutions resulting from oxygenations of (a) (**4**)Cu(CH_3CN) (40 mM) and (b) (**5**)Cu(CH_3CN) (10 mM) in THF at −80 °C, using $^{16}O_2$ (solid line) or $^{18}O_2$ (dashed line). The inset to plot (b) shows overtone bands. Excitation wavelengths were 457.9 and 514.5 nm, respectively. The asterisk indicates a solvent peak.

and has all of the rhomb (Cu_2O_2) and diketiminate heavy atoms in a common plane. Because this structure is predicted to be 3.4 kcal mol^{-1} higher in free energy than the D_2 minimum at 298 K, it makes little contribution to the experimental equilibrium, but it is interesting that it is predicted to be stable. The only local minimum structure found for **5** belongs to the C_2 point group and has a core structure resembling that of the bis(hydroxo)dicopper complex shown in Figure 4. In terms of metric data, the Cu−Cu distances in the bis(μ-oxo)dicopper complexes of **4** and **5** are predicted to be 2.860 and 2.783 Å, respectively, and the Cu−O distances are predicted to be 1.832 Å in **4** and 1.829 and 1.833 Å in **5** (where they are not required to be identical by symmetry). The substantially shorter Cu−Cu distance in **5** compared to **4** is attributable to the lack of substitution at the 2 and 4 positions of the formazan ring compared to the diketiminate. Thus, in **4**, the $CuNC_{ipso}$ angle, which describes the degree to which the aryl rings project forward from the diketiminate, is predicted to be 115.5°; in **5**, on the other hand, the corresponding angle is predicted to be 120.6°. The effect of this difference, which is experimentally shown (Figures 2−4 and S1 in the Supporting Information), is multiplied 2-fold upon dimerization, reducing unfavorable steric interactions associated with shorter Cu−Cu distances.

As a point of comparison that offers insight into the sensitivity of the Cu_2O_2 rhomb structure to electron-donating or -withdrawing groups on the ligands, the Cu−Cu and Cu−O distances in the bis(μ-oxo)dicopper complex of **3**, where the CF_3 groups in **4** are replaced by CH_3 groups, are predicted at the *m*PW1 level to be 2.836 and 1.831 Å, respectively. These values are quite similar to those for the bis(μ-oxo)dicopper complex of **4**, so the electron-withdrawing character of the CF_3 groups does not seem to have a particularly strong influence on the core rhomb structure. This observation is consistent with the experimental and predicted rR data. For the bis(μ-oxo)dicopper complex of **3**, the core breathing frequency is observed at 608 cm^{-1} ($\Delta^{18}O_2$ = 27 cm^{-1}).[5b] As shown in Figure 6, the corresponding frequency with **4** is at about 604 cm^{-1} if one assumes that the pair of peaks at 598 and 610 cm^{-1} result from a Fermi resonance. Theory provides some insights because predicted spectra are not complicated by the Fermi resonance phenomenon. For **3**, the breathing vibration is predicted at the *m*PW level to occur at 582 cm^{-1} with an $^{18}O_2$ isotope shift of 24 cm^{-1}, while for **4** the analogous values are 577 and 25 cm^{-1}. Thus, theory is consistent with an experimental assignment of the fundamental core frequency for the bis(μ-oxo)dicopper complex of **4** being only 4 or 5 cm^{-1} smaller than that of **3**

and showing an almost identical isotope shift.[39] The analogous frequencies in the bis(μ-oxo)dicopper complex of **5** are more difficult to assign because the totally symmetric breathing mode couples quite strongly with the aryl bending and formazan modes. One such frequency is predicted to be 565 cm^{-1} with an $^{18}O_2$ isotope shift of 20 cm^{-1}, and these values are roughly consistent with the *m*PW/experiment offsets for **3** and **4**, but the analysis in this case must be considered more tentative in the absence of a more sophisticated model that would include predicting rR intensities.

Having computed structures and energies for the bis(μ-oxo)dicopper and monocopper carbonyl complexes, we may also compute the energy changes for the reaction

$$2\mathrm{LCuCO} + \mathrm{O_2} \rightarrow [\mathrm{LCu}]_2(\mathrm{O})_2 + 2\mathrm{CO} \qquad (1)$$

At the *m*PW level, the computed 298 K free energies of reaction for this process are 25.4 and 9.9 kcal mol^{-1} for **4** and **5**, respectively. The bis(μ-oxo)dicopper species are not synthesized from the carbonyl compounds, but these values provide an indication of the differential stabilities of the two bis(μ-oxo)dicopper cores. The much greater stability of the complex with **5** compared to that with **4** may be traced to the reduced steric clash between the aromatic rings in the former, as noted above. As an interesting aside, we were successful in locating computationally a bis(μ-oxo)dicopper structure of **2** that was predicted to be a local minimum (belonging like **4** to the D_2 point group). However, the free energy of reaction for eq 1 with this ligand is predicted to be 45.6 kcal mol^{-1}, indicating how much more unfavorable the steric interactions between the isopropyl-substituted phenyl rings are compared to the methyl-substituted ones and rationalizing the failure to observe this dimerization experimentally.[6]

Turning last to the UV−vis spectra of the bis(μ-oxo)dicopper complexes of **4** and **5**, TD-DFT calculations using the B3LYP functional were analyzed to understand the nature of the longest-wavelength absorptions in these species. In the case of the complex with **4**, TD B3LYP predicts there to be only a single excitation having significant oscillator strength at low energy, and the wavelength of the transition is predicted to be 540 nm. This prediction is well to the red of the experimentally observed value, which is typical of CT excitations with TD B3LYP.[40] The transition itself is computed to be an excitation out of the antibonding π^* orbital formed from the out-of-plane O $2p_z$ orbitals (sometimes called the π_v^* orbital[20]) into an antibonding combination of Cu d_{xy} orbitals and the σ_u^* orbital formed by the antibonding combination of the O $2p_y$ orbitals along the O−O axis (Figure 7a). This excitation is exactly the same as that predicted by Estiú and Zerner, at the INDO/S level, to occur at lowest energy for a bis(μ-oxo)dicopper core supported by three imidazole ligands per Cu atom.[41] In the case of the complex with **4**, the donor orbital is predicted also to be substantially delocalized onto the diketiminate aryl rings, but the core contribution is dominated by the O−O π_v^*.

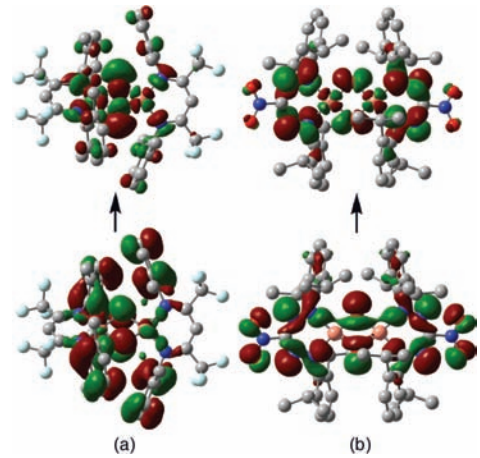

Figure 7. Predicted donor (below) and acceptor (above) Kohn−Sham molecular orbitals for the longest-wavelength transitions observed for the bis(μ-oxo)dicopper complexes of **4** (a) and **5** (b). The 0.02 au isodensity surfaces are visualized, and H atoms are removed for clarity. Cu atoms are peach, F atoms are aqua, O atoms are red, N atoms are blue, and C atoms are gray; the molecules are oriented with the Cu−Cu axis horizontal.

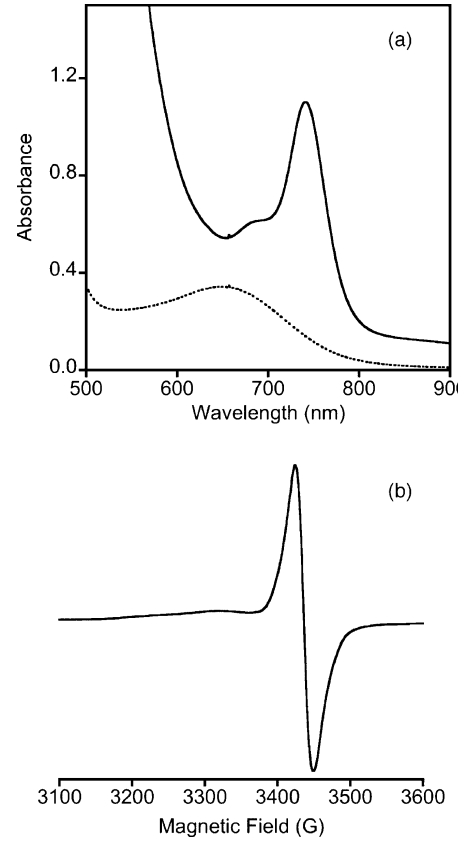

Figure 8. (a) UV−vis spectra of (**5**)Cu(CH_3CN) (dotted line) and the intermediate observed after oxygenation for 150 s at −10 °C in THF (solid line). (b) X-band EPR spectrum of the intermediate (4 K).

The most intense low-energy absorption for the bis(μ-oxo)dicopper complex with **5**, on the other hand, is predicted to occur at 548 nm at the TD B3LYP level and involves excitation from an occupied orbital comprised of the O $2p_y$ σ_u^* orbital and formazan in-plane ligand orbitals into the π_σ^* orbital, which is formed as an antibonding combination

(40) Cramer, C. J. *Essentials of Computational Chemistry: Theories and Models*, 2nd ed.; John Wiley & Sons: Chichester, U.K., 2004; pp 501−504.
(41) Estiú, G. L.; Zerner, M. C. *J. Am. Chem. Soc.* **1999**, *121*, 1893–1901.

Scheme 1

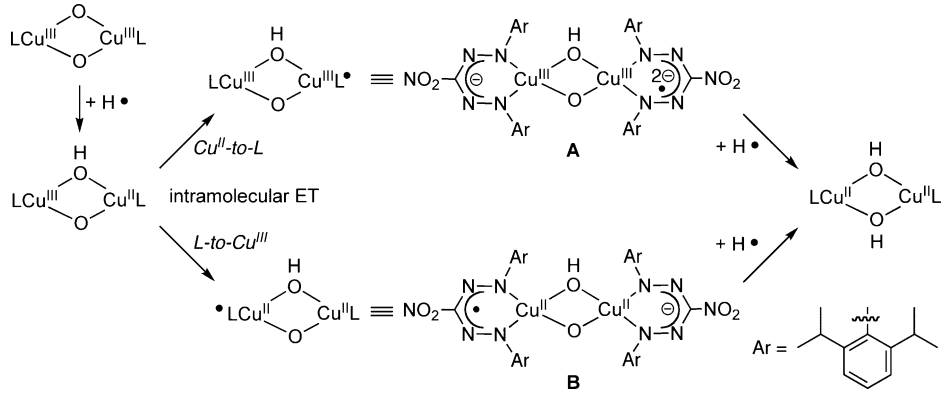

of the Cu d_{xy} orbitals and the O $2p_x$ π^* orbital (Figure 7b). This acceptor orbital also has a significant formazan π^* component. The excitation is very similar to that proposed by Henson et al. based on SCF-Xa-SW calculations for the lowest-energy excitation in a bis(μ-oxo)dicopper core supported by two ammonia ligands per copper.[36] In the case considered by Henson et al., however, there was substantial contribution to the occupied orbital by the Cu d_{xy} orbitals, while in this case, they are predicted to make negligible contribution to the occupied orbital. There is thus a more substantial overall CT character to this excitation that likely contributes to its intensity. The unique characteristics of the formazan ligand, with its framework orbitals lying at high energy in the occupied orbital manifold, are responsible for this interesting variation.

Decay of (5)$_2$Cu$_2$(μ-O)$_2$. As noted above, the UV−vis spectroscopic features of the bis(μ-oxo)dicopper complexes decayed upon warming above −80 °C, yielding $L_2Cu_2(OH)_2$ complexes that were isolated by performing the oxygenation at ambient temperature. Similar decompositions have been noted previously for bis(μ-oxo)dicopper compounds.[2,37] For the system supported by **5**, we observed an additional intermediate species during the decay process, the formation and decay of which was most conveniently monitored by performing the oxygenation of (**5**)Cu(CH_3CN) at temperatures above −50 °C. This new intermediate exhibits a narrow low-energy absorption feature at 742 nm ($\epsilon \sim 1100$ M^{-1} cm^{-1} per Cu; Figure 8a). While d−d transitions for copper(II) complexes often appear in this region of the UV−vis spectrum, such an assignment seems unlikely considering the band shape and intensity observed here. Kinetics experiments at −10 °C support a first-order rate law for both the formation ($k = 0.037$ s^{-1}) and decay ($k = 0.0024$ s^{-1}) of the 742 nm feature (Figure S3 in the Supporting Information). Measurements of the rates of formation in THF and THF-d_8 at −30 °C (Figure S4 in the Supporting Information) revealed a modest kinetic isotope effect (KIE = k_H/k_D) of 1.6, consistent with attack on the solvent C−H(D) bond during the conversion of the bis(μ-oxo)dicopper complex to the intermediate.[42] Most intriguing is the 4 K X-band EPR spectrum for the intermediate comprising an isotropic signal at $g \sim 2.0$ (Figure 8b), for which double integration indicates a total spin quantity of 77% relative to the bis(μ-oxo)dicopper precursor.

We hypothesize that the 742 nm absorption feature and the signal in the EPR spectrum arise from a species containing a ligand-centered radical. Scheme 1 depicts possible decomposition pathways to (**5**)$_2$Cu$_2$(OH)$_2$ via a proposed formazyl radical ligand intermediate (**A** or **B**).[12] Precedent for these formulations can be found in a related boron−formazan complex, which could be reduced to a "borataverdazyl" radical anion with similar spectroscopic features (a band at 738 nm in the solid-state electronic spectrum and an isotropic EPR signal at $g \sim 2.0$ in the solid state).[13] Furthermore, the acceptor orbital for (**5**)$_2$Cu$_2$(O)$_2$ (Figure 7) features significant contributions from formazan π^* orbitals that are analogous to the singly occupied molecular orbital of verdazyls, a well-established family of stable radicals.[43] Formulation **A** or **B** would result from an internal redox isomerization from an $L_2Cu^{III}Cu^{II}$ species, which would be the first product generated upon H-atom abstraction by the bis(μ-oxo)dicopper(III) complex (consistent with the observed KIE). The redox isomerizations concievably could involve electron transfer from the Cu^{II} site to the nitroformazan ligand or from the ligand to the Cu^{III} site to yield **A** or **B**, respectively. The former process to yield **A** would appear most likely, in view of the absence of any copper-based hyperfine splitting in the EPR signal and the fact that the borataverdazyl with analogous spectroscopic properties is generated by reduction rather than oxidation.[13] On the other hand, species **B** cannot be ruled out if strong antiferromagnetic coupling between the copper(II) centers and little if any coupling between those centers and the verdazyl radical are assumed.

Conclusions

Compared to copper(I) complexes of diketiminate ligands that feature alkyl or aryl backbone substituents (e.g., R′ = Me in Figure 1), those of ligands **4** and **5** feature electron-deficient metal centers, as best indicated by the high ν(CO) frequencies for the species LCu(CO). Nonetheless, the complexes LCu(CH_3CN) (L = **4** or **5**) react with O_2 at room

(42) Attempts to identify products of oxidation of the solvent via gas chromatography/mass spectrometry analysis after allowing the intermediate to decompose were unsuccessful, however.

(43) Gilroy, J. B.; McKinnon, S. D. J.; Kennepohl, P.; Zsombor, M. S.; Ferguson, M. J.; Thompson, L. K.; Hicks, R. G. *J. Org. Chem.* **2007**, *72*, 8062–8069.

temperature to yield bis(μ-hydroxo)dicopper complexes structurally defined by X-ray crystallography and at −80 °C to yield bis(μ-oxo)dicopper compounds, identified as such on the basis of UV−vis and rR spectroscopy, EPR silence, spectrophotometric titration data, and theory. The observation of bis(μ-oxo)dicopper complex formation upon low-temperature oxygenation of (**4**)Cu(CH_3CN) stands in contrast to the lack of O_2 reactivity reported previously for (**2**)Cu(CH_3CN), which is similarly electron-poor but is sterically more encumbered by virture of the diisopropylphenyl versus dimethylphenyl substituents. We surmise that in both cases O_2 binding is thermodynamically unfavorable, but in the case of the system with the less hindered **4**, rapid irreversible trapping of what is likely a small equilibrium concentration of a 1:1 adduct drives the reaction forward.

The nitroformazan ligand **5** confers unusual properties to its bis(μ-oxo)dicopper complex, such as an intense electronic absorption feature at lower energy than that seen previously[2,36] which is ascribed on the basis of theory to significant ligand orbital contributions to the $[Cu_2O_2]^{2+}$ core transition. In addition, the decay of $(\mathbf{5})_2Cu_2(\mu\text{-}O)_2$ proceeds via a novel observable intermediate that is assigned as a metalloverdazyl radical. We postulate that this radical species is formed by a mechanism involving H-atom abstraction from the solvent followed by an internal redox isomerization. Such an intramolecular electron transfer involving the formazan ligand may be viewed in the context of an extensive literature on redox noninnocent ligands and the novel reactivity of their complexes,[44] with reports of complexes containing aminyl ($R_2N^{\bullet}$) radical ligands generated by one-electron oxidation of the corresponding amido species being particularly relevant.[45] Thus, while structurally analogous to diketiminates, the formazan ligand system exhibits noninnocence and, as a result, alternate dimensions to its coordination chemistry.

Acknowledgment. We thank the NIH (Grant GM47365 to W.B.T.), NSF (Grant CHE-0610183 to C.J.C. and REU funds to B.D.N.), NSERC of Canada (R.G.H.), and UM Lando Undergraduate Research Program (B.D.N.) for financial support of this research. We also thank William Antholine for preliminary EPR data and analysis, J. D. Lipscomb and L. Que, Jr., for providing access to EPR and rR facilities, and Victor G. Young, Jr., for assistance with X-ray crystallography.

Supporting Information Available: X-ray crystallagraphic data in CIF format, tables of coordinates for calculated structures, and Figures S1−S5. This material is available free of charge via the Internet at http://pubs.acs.org.

IC9002466

(44) Selected recent examples:(a) Lu, C. C.; Bill, E.; Weyhermuller, T.; Bothe, E.; Wieghardt, K. *J. Am. Chem. Soc.* **2008**, *130*, 3181–3197. (b) Boyer, J. L.; Cundari, T. R.; DeYonker, N. J.; Rauchfuss, T. B.; Wilson, S. R. *Inorg. Chem.* **2009**, *48*, 638–645. (c) Ketterer, N. A.; Fan, H.; Blackmore, K. J.; Yang, X.; Ziller, J. W.; Baik, M.-H.; Heyduk, A. F. *J. Am. Chem. Soc.* **2008**, *130*, 4364–4374. (d) Blackmore, K. J.; Sly, M. B.; Haneline, M. R.; Ziller, J. W.; Heyduk, A. F. *Inorg. Chem.* **2008**, *47*, 10522–10532. (e) Stanciu, C.; Jones, M. E.; Fanwick, P. E.; Abu-Omar, M. M. *J. Am. Chem. Soc.* **2007**, *129*, 12400–12401.

(45) Hicks, R. G. *Angew. Chem., Int. Ed.* **2008**, *47*, 7393–7395, and references cited therein.